Chapter 1

Mathematical Model of the Mechanics and Dynamics of the Tails in Dinosaurs

Problem presented by: Donald Mackenzie (University of Calgary)

Mentors: C. Sean Bohun (Pennsylvania State University), Donald Henderson (University of Calgary), Bernard Monthubert (Institut de Mathématiques de Toulouse), Rex Westbrook (University of Calgary)

Student Participants: Robin Clysdale (University of Calgary), Diana David-Rus (Rutgers University), Matthew Emmett (University of Calgary), Chad Hogan (University of Calgary), Mark Hughes (University of Calgary), Enkeleida Lushi (Simon Fraser University), Peter Smith (Memorial University of Newfoundland), Naveen Vaidya (York University)

Report prepared by: C. Sean Bohun (csb15@psu.edu)

1.1 Introduction

Unlike mammals which have very reduced tails, the tails of dinosaurs represented a substantial fraction of their body lengths and masses. The left and right sides of the tail base in all dinosaurs acted as the anchor points for large, powerful muscles that attached on the rearward side of the hind limbs (Figure 1.1). These muscles pulled on the legs, causing them to rotate backwards and under the body, with the result that the animals were propelled forward. As well as pulling on the legs, these muscles would have exerted a reciprocal pull on the tail. During locomotion the left and right hind limbs would be alternately pulled, and be 180° out of phase with each other. These alternating tugs would have set up oscillations in the tail. It would seem that some sort of synchrony would have to arise between the rate at which the legs were swung back and forth and the natural frequencies of oscillations of the tail to allow efficient, stable walking and running. The extreme sizes of some dinosaurs—up to 30 tonnes in some cases—and the great range of body sizes—from a few hundred grams to many tonnes—gives dinosaurs the potential to be insightful models for the study of locomotory dynamics in terrestrial animals.

There are two possible avenues to investigate the effects of tails on locomotion:

1. Focus on just the ~ 14m tail of Diplodocus carnegii, a 24m sauropod where the tail represents approximately 26% of the total body mass detailed in Figure 1.2.

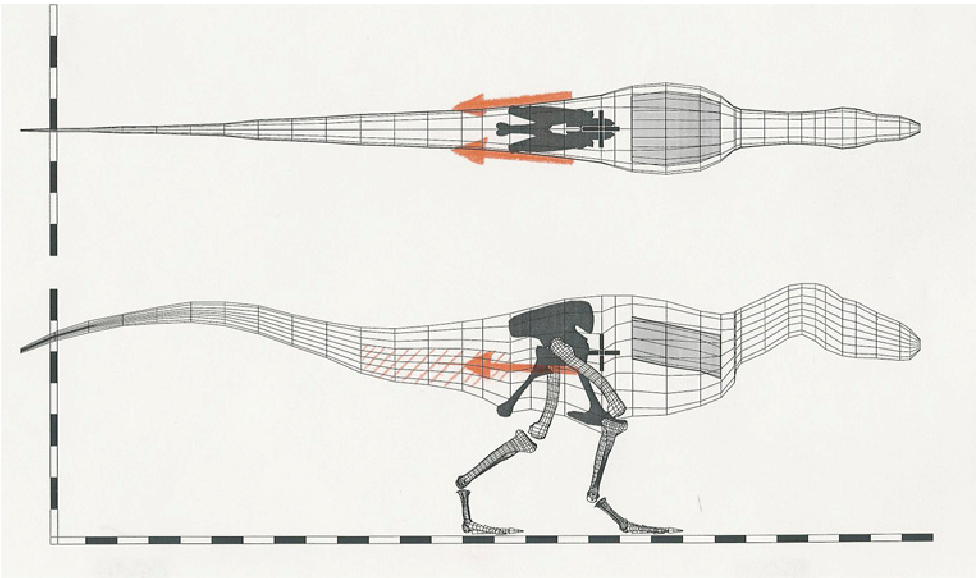

Figure 1.1: Anatomical details of the tail base structure in dinosaurs.

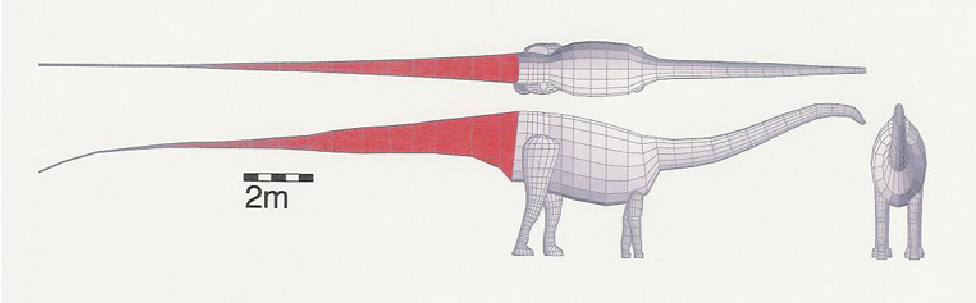

Figure 1.2: Diplodocus carnegii is a 24m sauropod with a 14m long tail.

2. Investigate the variation in tail mechanics that occurred during the evolution of theropod dinosaurs—the two-legged, carnivores. In small, early theropods such as the 30cm long Compsognathus the tail represents just over half the total body length, and is very slender and flexible. In larger, later theropods such as a 12m Tyrannosaurus the tail represents just one third of the total body length, and is proportionally deeper and much stiffer. Figure 1.3 illustrates this variation in tail structure.

Section 1.2 begins with a survey of physical data for both bipedal and quadrupedal dinosaurs. In this section the ratio of the tail to leg length is compared across many diverse species and a scaling law is developed that relates the tail length, leg length and tail radius. A continuous model for the tail is developed in Section 1.3 and by nondimensionalising a small parameter related to the thinness of the tail simplifies the resulting coupled nonlinear equations. It is shown that the resulting set of equations contain aspects of both beam dynamics and wave propagation. In Section 1.4 a discrete version of the tail is derived with the assumption that the sections of the tail are coupled with a stiff joint that allows

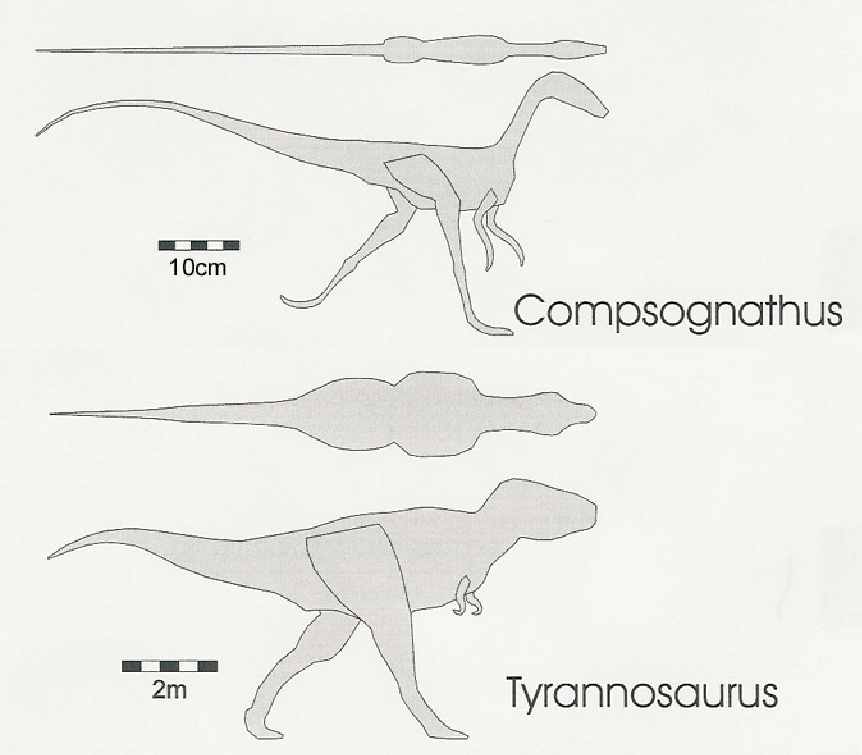

Figure 1.3: Comparison of the tail structures for Compsognathus and Tyrannosaurus.

rotation but does not allow extension. In this model the stiffness of each joint is characterized by an effective spring constant k_i for the ith joint and results in a discrete version of the Euler-Bernoulli expression for each of the tail segments. The paper finishes with some preliminary conclusions and directions for future work.

1.2 Dimensional Analysis

As a first model we suppose that the tail acts like a flexible beam with the periodic driving force of the rear legs modelled with a pendulum. If the beam has length L_{tail} and effective radius R_{tail} then the deflection of the beam $u(x,t) : [0, L_{\text{tail}}] \times [0,\infty) \to \mathbb{R}$ is given by

$$\frac{\partial^2}{\partial x^2}\left(EI(x)\frac{\partial^2 u}{\partial x^2}\right) = \rho A(x)\frac{\partial^2 u}{\partial t^2}$$

where E is the Young's modulus, I is the moment of inertia about the neutral axis, ρ is the density, and A is the cross section of the tail. If we nondimensionise by substituting

$$\hat{x} = \frac{x}{L_{\text{tail}}}, \qquad \hat{u} = \frac{u}{L_{\text{tail}}}, \qquad \hat{t} = \frac{t}{T_{\text{tail}}},$$
$$I = R_{\text{tail}}^4 \hat{I}, \qquad A = R_{\text{tail}}^2 \hat{A}$$

we find that

$$\frac{ER_{\text{tail}}^2 T_{\text{tail}}^2}{\rho L_{\text{tail}}^4} \frac{\partial^2}{\partial \hat{x}^2}\left(\hat{I}\frac{\partial^2 \hat{u}}{\partial \hat{x}^2}\right) = \hat{A}\frac{\partial^2 \hat{u}}{\partial \hat{t}^2}.$$

This indicates that the characteristic time to propagate a disturbance the complete length of the tail is

$$T_{\text{tail}} \sim \left(\frac{\rho}{E}\right)^{1/2} \frac{L_{\text{tail}}^2}{R_{\text{tail}}}.$$

At the same level of approximation assume that the legs of the dinosaur act like a pendulum of length L_{leg} so that the characteristic period for the motion of the legs is on the order of

$$T_{\text{leg}} \sim \left(\frac{L_{\text{leg}}}{g}\right)^{1/2}$$

where g is the acceleration due to gravity. As a result, if the tail plays a significant role in the locomotion with this model then $T_{\text{leg}} \sim T_{\text{tail}}$ and

$$\frac{L_{\text{tail}}^4}{L_{\text{leg}} R_{\text{tail}}^2} = \text{const.} \tag{1.1}$$

depending only on the composition of the tail. Notice that this expression predicts that for a fixed leg length, increasing the length of the tail necessarily increases its effective radius in contrast with the archaeological evidence.

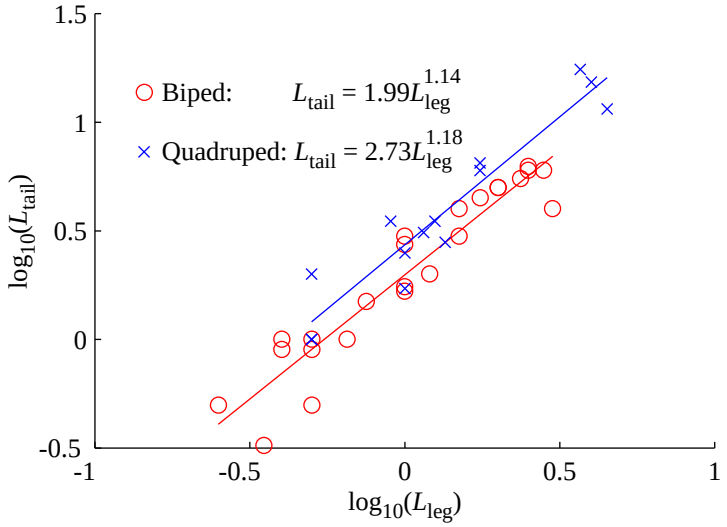

Figure 1.4: L_{tail} as a function of L_{leg} for a sample of bipedal and quadrupedal dinosaurs.

Figure 1.4 compares approximate values of the leg length to the tail length for a selection of bipedal and quadrupedal dinosaurs. For bipeds, the tail is typically twice the length of the leg whereas in quadrupeds the tail is, on average, an additional 40% longer. Figure 1.5 illustrates expression (1.1)

and contrasts it with an optimal expression that minimizes the variation. Clearly the beam/pendulum model is not reflected in the sample but the variance is drastically reduced with the expressions

$$\text{Bipeds: } \frac{L_{\text{tail}}^{0.45} R_{\text{tail}}^{0.39}}{L_{\text{leg}}} = \text{const.} \qquad \text{Quadrupeds: } \frac{L_{\text{tail}}^{0.23} R_{\text{tail}}^{0.69}}{L_{\text{leg}}} = \text{const.} \tag{1.2}$$

These results imply that for a fixed leg length, if the length of the tail is doubled then the radius of the tail in a biped is halved, whereas in a quadruped the radius of the tail is reduced to one-eighth of its original value. So we see that bipeds tend to have much thicker tails than correspondingly sized quadrupeds.

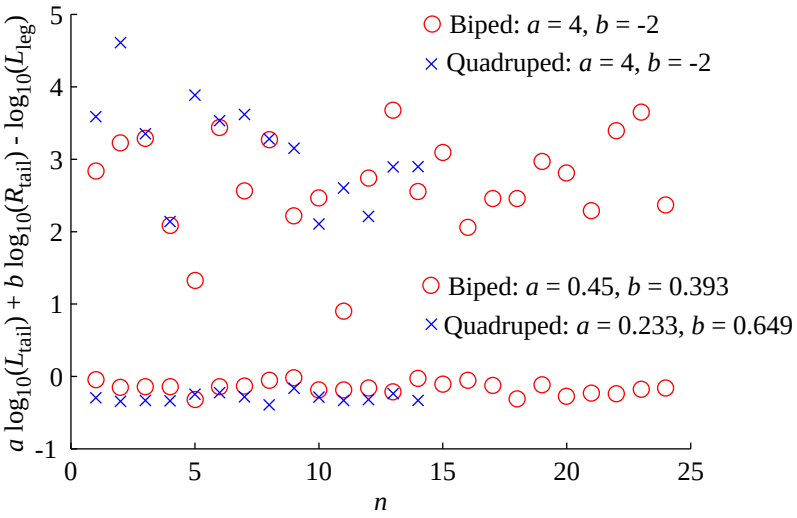

Figure 1.5: Scatter plot of the data assumed to satisfy (1.1) and the corresponding plot of the data when a and b are chosen to minimize the variance.

The question remains to find a mechanism that predicts the archaeological evidence described in (1.2). In the case of bipeds a similar expression can be recovered by analysing the simple cantilever depicted in Figure 1.6. Here the tail, rear legs, and forward torso are replaced with rectangular blocks. The condition that this effective dinosaur does not tip over is $L_{\text{leg}}^2(L_{\text{leg}}/2) - 2L_{\text{tail}}R_{\text{tail}}(L_{\text{tail}}/2) = 0$ or

$$\frac{L_{\text{tail}}^{2/3} R_{\text{tail}}^{1/3}}{L_{\text{leg}}} = \text{const.}$$

the point here is that scaling expressions like (1.2) are a result of balance equilibrium rather than synchronous locomotion. So it seems more likely that the physical dimensions of the tail are chosen to balance the dinosaur rather than complementing its locomotion dynamics.

1.3 Inextensible Rod Equations

We turn the discussion to the development of an appropriate model for the tail of the dinosaur and we begin with a derivation of the equations satisfied by an inextensible rod.

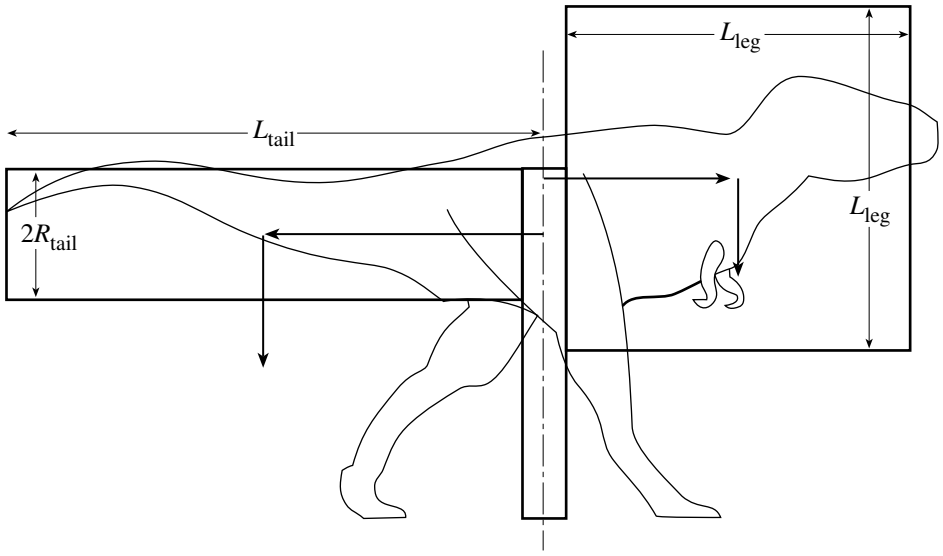

Figure 1.6: An effective dinosaur with the major anatomical structures replaced with blocks of a representative size.

To the left of Figure 1.7 is a segment of length Δs with orientation ϕ, internal tensions of F, G in the x, y directions, a bending moment M and an external force of $\vec{P}$ per unit length. In this case we are viewing the tail from above so that $\vec{P}$ is essentially zero since the weight of the tail acts perpendicular to this plane. It is simply left in for completeness. In any case, simple geometry gives the relationships

$$\cos\phi = \Delta x/\Delta s, \qquad \sin\phi = \Delta y/\Delta s. \tag{1.3}$$

If the density and cross sectional area of the segment are ρ and A respectively then the mass of the segment is $\rho A\Delta s$ and by resolving the linear motion in the x and y directions one obtains

$$(\rho A\Delta s)x_{tt} = \Delta F + P_1\Delta s, \qquad (\rho A\Delta s)y_{tt} = \Delta G + P_2\Delta s. \tag{1.4}$$

The angular motion is given by $I_0\phi_{tt} = \tau$ where I_0 is the moment of inertia of the cross section and τ is the net torque acting on the segment. From Figure 1.7, taking torques about the point A, one finds that $\tau = \Delta M - F\Delta y + G\Delta x$ so that

$$(\rho I\Delta s)\phi_{tt} = \Delta M - (F\Delta s)\sin\phi + (G\Delta s)\cos\phi \tag{1.5}$$

where we have used the moment of inertia of the cross section defined as

$$I = \iint_A y^2\, dA.$$

This quantity is analogous to the ordinary moment of inertia I_0 except that the mass element is replaced by the area element of the cross section. Note that the torque due to the external force is of a higher order of smallness.

A final relationship can be obtained by assuming that the amount of bending is small and that the material satisfies a linear constitutive relation $\sigma = E\epsilon$ relating the stress to the strain. Referring to the

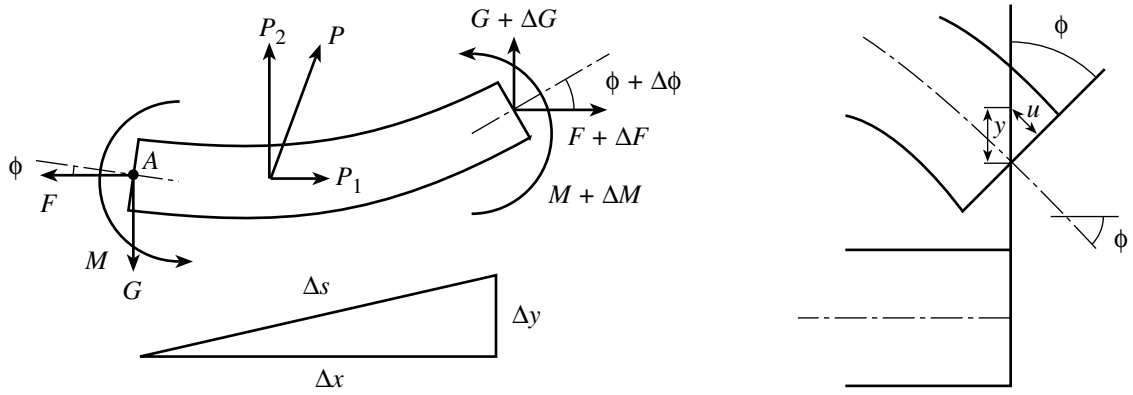

Figure 1.7: To the left a rod segment of length Δs experiences internal forces of F, G, a bending moment M and an external force per unit length of $\vec{P}$. To the right a portion of the rod is bent through an angle ϕ. If the normal to the cross section remains normal, the displacement $u = y\phi$.

right of Figure 1.7, a section of rod is bent through an angle ϕ. If this angle is sufficiently small then the normal to the cross section will remain normal after the bending distortion and the the displacement of the rod as a function of the distance from the neutral line is given by $u = y\phi$. Since the bending moment M for a given cross section is the sum of the moments about the neutral plane $y = 0$ these assumptions give the relationship

$$M = \iint_A y\sigma \, dA = E \iint_A y\epsilon \, dA = E\phi_s \iint_A y^2 \, dA = EI\phi_s. \tag{1.6}$$

In this expression σ is the stress in the rod, and $\epsilon = du/ds$ is the corresponding strain. Equation (1.6) is occasionally referred to as the Euler-Bernoulli assumption.

Letting the length of the segment Δs shrink to zero gives the final set of equations satisfied by an inextensible rod

$$x_s = \cos\phi, \tag{1.7a}$$
$$y_s = \sin\phi, \tag{1.7b}$$
$$\rho A x_{tt} = F_s + P_1, \tag{1.7c}$$
$$\rho A y_{tt} = G_s + P_2, \tag{1.7d}$$
$$\rho I \phi_{tt} = M_s - F\sin\phi + G\cos\phi, \tag{1.7e}$$
$$M = EI\phi_s. \tag{1.7f}$$

To nondimensionalise we assume that there is a circular cross section so that the radius $R = R_0 r(s)$, $A = \pi R_0^2 r^2$, and $I = \pi R_0^4 r^4/4$. Scaling the lengths with the length of the tail L we let

$$\hat{x} = \frac{x}{L}, \qquad \hat{y} = \frac{y}{L}, \qquad \hat{s} = \frac{s}{L}, \qquad \hat{t} = \frac{t}{T},$$
$$\hat{F} = \frac{F}{K}, \qquad \hat{G} = \frac{G}{K}, \qquad \hat{M} = \frac{M}{LK}, \qquad \hat{P}_i = \frac{P_i}{K}$$

and identify three nondimensional quantities $C_1 = \pi\rho R_0^2 L^2/KT^2$, $C_2 = \pi\rho R_0^4/4KT^2$ and $C_3 = 4KL^2/\pi E R_0^4$. The characteristic magnitudes of the force and time should reflect the physical properties of the tail. Consider a rod of length L which is clamped horizontally at one end, free at the other, and bends under its own weight. If the rod has mass m and g is the gravitational constant then the shape satisfies

$$\zeta^{(iv)} = \frac{mg/L}{EI}, \qquad \zeta(0) = \zeta'(0) = \zeta''(L) = \zeta'''(L) = 0,$$

with solution

$$\zeta(s) = \frac{mg/L}{24EI} s^2(s^2 - 4Ls + 6L^2)$$

and a maximum displacement at $s = L$ that satisfies

$$\frac{\zeta(L)}{L} = \frac{1}{8}\,\frac{mg}{L^2/EI}.$$

In this case the characteristic force for a rod that bends under its own weight is $K = EI/L^2$ and choosing this value for K sets $C_3 = 1$. This leaves two natural choices for T. Either $T = L\sqrt{\rho/E}$ or $T = 2L^2\sqrt{\rho/E}/R_0$ in which $C_2 = 1$ or $C_1 = 1$ respectively. We choose the latter consequently

$$T^2 = \frac{4\rho\pi L^4}{ER_0^2} = \frac{\rho\pi R_0^2 L^4}{EI},$$

$C_1 = 1$, and $C_2 = (R_0/2L)^2$ is a small parameter for a long thin tail and is denoted as ϵ.

Dropping hats the nondimensional equations are

$$x_s = \cos\phi, \tag{1.8a}$$
$$y_s = \sin\phi, \tag{1.8b}$$
$$r^2(s)x_{tt} = F_s + P_1, \tag{1.8c}$$
$$r^2(s)y_{tt} = G_s + P_2, \tag{1.8d}$$
$$\epsilon r^4(s)\phi_{tt} = M_s - F\sin\phi + G\cos\phi, \tag{1.8e}$$
$$M = r^4(s)\phi_s \tag{1.8f}$$

with $0 \le s \le 1$, and $r(s) = R(s)/R_0$ a nondimensional radius of the rod. Since ϵ is small, equation (1.8e) implies that if initially $\tau(s) = M_s - F\sin\phi + G\cos\phi \neq 0$ then ϕ will change rapidly with time until $\tau = 0$. Conversely, equations (1.8c) and (1.8d) indicate that x and y will not appreciably change during this equalization process. On the time scale of T, the ϵ term can be omitted and expression (1.8e) can be replaced with

$$\tau(s) = M_s - F\sin\phi + G\cos\phi = 0.$$

1.3.1 Boundary Conditions and Initial Conditions

Since the tip of the tail $(s = 1)$ is free, the internal forces and bending moments vanish so that $F = G = M = 0$. At the base $(s = 0)$ it is not clear if one should consider a clamped, hinged, or

simply supported condition. For a clamped base both the position and direction are specified fixing $x(t,0)$, $y(t,0)$, $x_s(t,0)$, and $y_s(t,0)$ for all t. If the base is hinged then the position is fixed but the bending moment M is zero. Finally, if the base is supported then it is free to slide and both the point of contact and the direction are unknown. In this final case $M = 0$ and the direction of vector $\langle F, G\rangle$ must be perpendicular to the rod.

By initially assuming that the tail is in equilibrium and that there is no external forces acting on the tail in the xy-plane ($P_1 = P_2 = 0$) we find that $F_s = G_s = 0$ so that both $F(0,s) = F_0$ and $G(0,s) = G_0$ are constant. Since F and G are constant, the condition $\tau = 0$ can be integrated to give $M(0,s) = x(s)G_0 - y(s)F_0$ to avoid any fast dynamics.

1.3.2 Small Deflection Approximation

Suppose that the lateral deflection is small so that $\phi \simeq 0$, $P_1 = P_2 = 0$ and (1.8a)-(1.8f) become with $\epsilon = 0$

$$\begin{aligned} x_s &= 1, & y_s &= \phi, \\ r^2(s)x_{tt} &= F_s, & r^2(s)y_{tt} &= G_s, \\ M_s &= F\phi - G, & M &= r^4(s)\phi_s. \end{aligned}$$

This implies that the x co-ordinate of the rod coincides with the arc length, $x = s$, and the bending moment $M = r^4(s)y_{ss}$. Therefore

$$G_s = F_s\phi + F\phi_s - M_{ss} = r^2(s)x_{tt}y_s + Fy_{ss} - (r^4(s)y_{ss})_{ss} = r^2(s)y_{tt}$$

or by setting $x(t,s) = s$,

$$Fy_{xx} - (r^4(x)y_{xx})_{xx} = r^2(x)y_{tt}. \tag{1.9}$$

If the tension in the x direction $F = 0$, as we expect near the tip of the tail, then the deflection y satisfies

$$(r^4(x)y_{xx})_{xx} + r^2(x)y_{tt} = 0$$

which is the beam equation. Alternatively if the bending moment M and tension F are constant then

$$Fy_{xx} = r^2(x)y_{tt}$$

which is the wave equation satisfied by a string under tension. In this small deflection limit, aspects of both the wave and beam equations are contained in this inextensible rod model.

1.4 Discrete Block Model

Rather than a continuous tail, we can simplify the model by supposing that the tail consists of a finite sequence of N discrete blocks that are connected by a stiff joint that allows rotation but no normal displacement. The geometry and the applied forces are indicated in Figure 1.8.

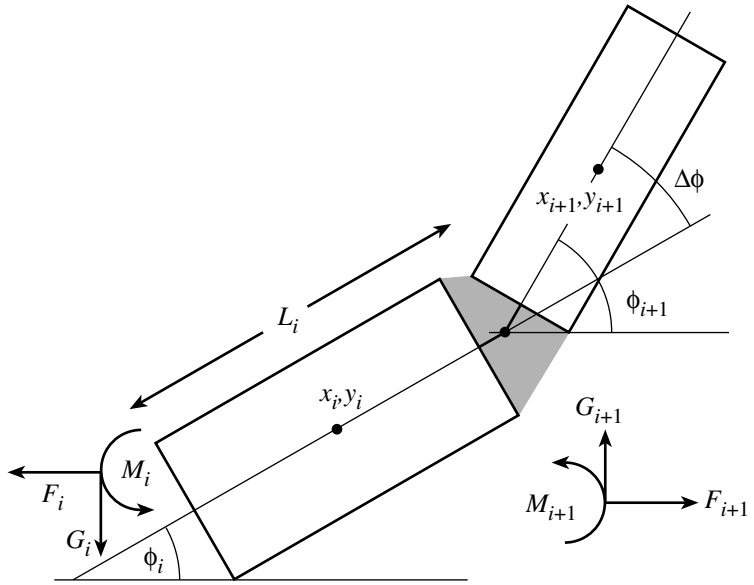

Figure 1.8: Each block is characterized by a mass of $\rho A_i L_i$ where A_i and L_i are the cross sectional area and the length of the ith block. Forces and moments F_i, G_i, M_i act to the left of the ith black and the segments are connected to one another by a stiff joint that allows rotation but no extension. The grey area can be thought of as a uniform distribution of collagen springs with a spring constant k_i.

The co-ordinates of the centre of mass of block $i+1$ is given by

$$x_{i+1} = x_i + \frac{L_i}{2}\cos\phi_i + \frac{L_{i+1}}{2}\cos\phi_{i+1}, \qquad i = 1, 2, \ldots, N-1$$
$$y_{i+1} = y_i + \frac{L_i}{2}\sin\phi_i + \frac{L_{i+1}}{2}\sin\phi_{i+1}, \qquad i = 1, 2, \ldots, N-1$$

and the origin is taken so that $x_1 = y_1 = 0$. In a similar fashion the net force and bending moment acting on block i give for $i = 1, 2, \ldots, N-1$

$$\rho A_i L_i \ddot{x}_i = F_{i+1} - F_i,$$
$$\rho A_i L_i \ddot{y}_i = G_{i+1} - G_i,$$
$$\rho I_i L_i \ddot{\phi}_i = M_{i+1} - M_i - \frac{L_i}{2}(F_{i+1} + F_i)\sin\phi_i + \frac{L_{i+1}}{2}(G_{i+1} + G_i)\cos\phi_i,$$

where the dots denote differentiation with time. For $i = N+1$, $L_{i+1} = 0$ and we choose $F_{N+1} = G_{N+1} = M_{N+1} = 0$ since the last block has a free end. These are simply a discretised version of the original extension free equations (1.7a)-(1.7f). What remains is a discrete version of the Euler-Bernoulli expression relating the bending moment to the curvature of the tail.

Suppose that there is a uniform distribution of collagen springs in the gap between blocks i and $i+1$. Let k_i denote the spring constant measured so that a uniform displacement of length l_i, the springs equilibrium length, generates a restoring force of $-k_i$. In this case the units of k_i is force/area rather than the standard force/length. If we instead suppose there is an angular displacement of $\phi_{i+1} - \phi_i =$

$\Delta\phi \neq 0$ then the springs on one side of the pivot are compressed and the springs on the other side are stretched from their equilibrium length. Each of the springs contributes a force $F = -k_i x \Delta\phi / l_i$ where x is the distance of a given spring from the pivot point and the total force is

$$F_{\text{tot}} = -\iint_A \frac{k_i \Delta\phi}{l_i} x \, dA = 0$$

so that the internal forces are not modified by the rotation of $\Delta\phi$.

The bending moment does changes since

$$M_i = \iint_A xF \, dA = \iint_A \frac{k_i \Delta\phi}{l_i} x^2 \, dA = \frac{k_i I_i \Delta\phi}{l_i} \tag{1.10}$$

where I_i is the moment of inertia of the cross section of block i. If we compare this with a discrete version of the Euler-Bernoulli expression we have

$$M_i = E_i I_i \frac{\Delta\phi}{\Delta s} = E_i I_i \frac{\Delta\phi}{(L_i/2 + L_{i+1}/2)}) = \frac{k_i I_i \Delta\phi}{l_i}.$$

So we see that equation (1.10) is a discrete version of the Euler-Bernoulli expression with an elastic modulus of

$$E_i = \frac{k_i}{2l_i}(L_i + L_{i+1})$$

consistent with a stress of magnitude k_i generating a strain of $l_i/(L_i/2 + L_{i+1}/2)$.

In summary the discrete block solution must satisfy for $i = 1, 2, \ldots, N-1$

$$x_{i+1} = x_i + \frac{L_i}{2}\cos\phi_i + \frac{L_{i+1}}{2}\cos\phi_{i+1}, \tag{1.11a}$$

$$y_{i+1} = y_i + \frac{L_i}{2}\sin\phi_i + \frac{L_{i+1}}{2}\sin\phi_{i+1}, \tag{1.11b}$$

$$\rho A_i L_i \ddot{x}_i = F_{i+1} - F_i, \tag{1.11c}$$

$$\rho A_i L_i \ddot{y}_i = G_{i+1} - G_i, \tag{1.11d}$$

$$\rho I_i L_i \ddot{\phi}_i = M_{i+1} - M_i - \frac{L_i}{2}(F_{i+1} + F_i)\sin\phi_i + \frac{L_{i+1}}{2}(G_{i+1} + G_i)\cos\phi_i, \tag{1.11e}$$

$$M_i = \frac{k_i I_i}{l_i}(\phi_{i+1} - \phi_i) \tag{1.11f}$$

where the $\ddot{x}_i$ and $\ddot{y}_i$ in the third and fourth expressions must be consistent with the first two expressions. Furthermore, the internal tension and moments of the first block F_1, G_1, M_1 should be chosen to emulate the time dependent forces that the hip exerts on the tail and $F_N = G_N = M_N = 0$ at the free end of the tail.

1.5 Conclusion

Having considered a cross section of both bipedal and quadrupedal dinosaurs we found that the scaling laws give a first indication that the proportions are typically chosen to balance the dinosaur as opposed to acting as an aid to locomotion.

Two models for the motion of the tail were explored. The first of these was a continuous model and for small deflections it was shown to include aspects of the dynamics of a thin beam as well as the dynamics of wave motion. This is very encouraging since both of these behaviours are seen in the tails of modern day animals. Unfortunately the resulting equations are a set of strongly coupled partial differential equations and more time is required to fully develop a solution consistent with the mass distribution of a given dinosaur.

To simplify the situation a discrete version of the continuous model was developed where the tail is broken into N blocks joined together with a stiff connection that allows rotation but no extension. Once again the result is a set of strongly coupled equations, but there is improvement. First, we are left with ordinary differential equations and second, the Euler-Bernoulli equation in the continuous model is recovered in the discrete model as a result of the behaviour of the springs in each joint. In some sense this result is not really unexpected since the discrete model is simply the continuous model written as a numerical implementation of the method of lines.

The next step is to simulate the motion of a tail predicted with the discrete block model for a living animal to estimate the model predictability. Choosing many segments for the tail of varying stiffness ($E_{\text{bone}} \simeq 20$GPa, $E_{\text{collagen}} \simeq 1$GPa) should produced reasonable dynamics. Once this has been accomplished, one can assess the degree to which a tail would have aided in the locomotion of pedal and quadrupedal dinosaurs.

1.6 Acknowledgements

The authors would like to acknowledge the Pacific Institute for the Mathematical Sciences (PIMS) for their sponsorship of the IPSW. We would also like to take this opportunity to thank the University of Calgary hospitality in hosting this event and special thank-you is reserved for Elena Braverman and Marian Miles. Their hard work and dedication ensured the success of the workshop.

Bibliography

[1] Berger, S.A., Goldsmith, E.W. & Lewis, E.R. (2000). *Introduction to Bioengineering.* Oxford University Press.

[2] Chouaieb, N. & Maddocks, J.H. (2004). Kirchhoff's problem of helical equilibria of uniform rods. *Journal of Elasticity.* **77**, pp. 221-247.

[3] Coleman, B.D., Tobias, I. & Swigon, D. (1995). Theory of the influence of end conditions on self-contact in DNA loops. *Journal of Chemical Physics.* **103**(20), pp. 9101-9109.

[4] Dill, E.H. (1992). Kirchhoff's theory of rods. *Archive for History of Exact Sciences.* **44**(1), pp. 1-23.

[5] Goriely, A. & Tabor, M. (2000). The nonlinear dynamics of filaments. *Nonlinear Dynamics.* **21**, pp. 101-133.

[6] Landau, L.D. & Lifshitz, E.M. (1970). *Theory of Elasticity*, 2nd ed. Pergamon Press: New York.

[7] Nizette, M. & Goriely, A. (1999). Towards a classification of Euler-Kirchhoff filaments. *Journal of Mathematical Physics.* **40**(6), pp. 2830-2866.

[8] Swigon, D., Coleman, B.D. & Tobias, I. (1998). The elastic rod model for DNA and its application to the tertiary structure of DNA minicircles and mononucleosomes. *Biophysical Journal.* **74**, pp. 2515-2530.

[9] Tam, D., Radovitzky, R. & Samtaney, R. (2005). An algorithm for modelling the interaction of a flexible rod with a two-dimensional high-speed flow. *International Journal for Numerical Methods in Engineering.* **64**(8), pp. 1057-1077.

[10] Tobias, I., Swigon, D. & Coleman, B.D. (2000). Elastic stability of DNA configurations. I. General theory. *Physical Review E.* **61**(1), pp. 747-758.

[11] Woodall, S.R. (1966). The large amplitude oscillations of a thin elastic beam. *International Journal of Non-linear Mechanics.* **1**, pp. 217-238.

[12] Animated dinosaurs:
`http://palaeo.gly.bris.ac.uk/dinosaur/animation.html`

[13] Anatomical data:
`http://internt.nhm.ac.uk/jdsml/nature-online/dino-directory/datafiles.dsml`

[14] Dinosaur support information:
`http://www.ucmp.berkeley.edu/diapsids/saurischia/saurischia.html`

`http://www.ucmp.berkeley.edu/diapsids/ornithischia/ornithischia.html`

`http://www.enchantedlearning.com/subjects/dinosaurs/index.html`